Applied Catalysis B: Environmental 183 (2016) 291–297

Contents lists available at ScienceDirect

Applied Catalysis B: Environmental

journal homepage: www.elsevier.com/locate/apcatb

Enhanced generation of reactive oxygen species for efficient pollutant elimination catalyzed by hemin based on persistent free radicals

Bin Jiang [a], Yuyuan Yao [a,*], Renjie Xie [a], Dejun Dai [a], Wangyang Lu [a], Wenxing Chen [a], Li Zhang [b]

[a] National Engineering Lab of Textile Fiber Materials & Processing Technology (Zhejiang), Zhejiang Sci-Tech University, Hangzhou 310018, PR China
[b] The School of Material Science and Chemical Engineering, Ningbo University, Ningbo 325211, PR China

ARTICLE INFO

Article history:
Received 12 August 2015
Received in revised form 25 October 2015
Accepted 28 October 2015
Available online 31 October 2015

Keywords:
Persistent free radicals
Multiwalled carbon nanotubes
Hemin
Reactive oxygen species

ABSTRACT

Porphyrin has received increasing interest in the catalysis field due to their excellent catalytic performance, nevertheless, the development of highly efficient porphyrin catalysts is still a significant challenge. In this work, a representative of persistent free radicals (PFRs), multiwalled carbon nanotubes (MWCNTs), was innovatively employed to construct an outstanding catalytic system, hemin-MWCNTs/H_2O_2. The introduction of MWCNTs greatly enhanced the catalytic activity of hemin, representing about 61 times higher reaction rate constant with the dye of methylene blue (MB) as probe compound, which was attributed to more reactive oxygen species (ROS) (•OH and hemin (Fe^{IV}=O)) generation. When MWCNTs were introduced to hemin/H_2O_2 system, the decrease of PFRs concentration in MWCNTs were observed with larger number of trapped electrons, indicating that PFRs might transfer electrons to hemin, thus speeding up the reaction rate-determining step of hemin (Fe^{III}) to hemin (Fe^{II}), resulting in enhanced production of •OH and hemin (Fe^{IV}=O). This study initiates an up-to-date research domain of PFRs-enhanced catalysis, paving the avenue toward developing robust processes for the efficient generation of ROS for applications in catalysis field.

1. Introduction

Hemin is a biologically active iron-porphyrin compound with peroxidase-like activity and high catalytic performance, which has attracted considerable attention in the catalysis field [1–4]. However, direct application of hemin as molecular catalysts is still of significant challenge due to its molecular aggregation in aqueous solution to form catalytic inactive dimers, which causes passivation of its catalytic activity [5–7]. To overcome these problems, two alternative strategies have been formulated. One strategy is to decorate the porphyrin macrocycle with bulky functional groups to protect the iron porphyrin centers [8]. This strategy, however, is limited by the difficulty of synthesizing these porphyrins [9]. Another alternative strategy is to use high surface area materials, such as titanium dioxide [10], montmorillonite [11], β-cyclodextrin [12], hydrogel [13] to support hemin to achieve improved stability and activity [14]. Although these hemin-based catalysts have shown better catalytic activity than free hemin in aqueous solutions, which is, however, still not high enough.

It is noteworthy that the catalytic activity of hemin mainly depends on the behavior of electron donation and acceptance between central iron and reactants. Therefore, changing the rate of electron transfer during the oxidation process might influence the catalytic performance of hemin. Recently, it has been reported that some resonance-stabilized radicals, also referred as persistent free radicals (PFRs) could act as electron donor, which can sustainably provide electrons to other electron-acceptors such as various oxidants and higher valent metals [15,16]. This excellent property might feature the capability to accelerate some important catalytic redox processes such as iron-mediated cycle involved the intrinsic drawback of slow iron reduction rate to generate ROS. Therefore, PFRs may find promising application in enhancing the catalytic activity of hemin.

Some studies have suggested that carbonaceous materials contain PFRs, which gradually received attention in catalysis field [17,18]. Therefore, the introduction of carbonaceous materials to hemin system may accelerate electron transfer to hemin to promote the catalytic efficiency due to the role of PFRs. Among carbonaceous materials, carbon nanotubes (CNTs) pos-

* Corresponding author. Fax: +86 571 86843255.
E-mail address: yyy0571@126.com (Y. Yao).

http://dx.doi.org/10.1016/j.apcatb.2015.10.051
0926-3373/

sess outstanding physical properties, excellent chemical stability, mechanical strength and high surface area [19–21]. Moreover, unsaturated π-system of CNTs could enhance the efficiency of electron transfer between CNTs and hemin due to π-stacking interactions [22]. Herein, multiwalled carbon nanotubes (MWCNTs), a representative of PFRs, were used to support hemin covalently to obtain a heterogeneous catalyst (hemin-MWCNTs). To our best of knowledge, reports about hemin-MWCNTs directly as oxidation catalysts and a detail understanding of the role of PFRs in MWCNTs is lacking.

The aim of this study was to investigate the catalytic activity of hemin-MWCNTs, and to reveal the role of PFRs during the catalytic oxidation process. Methylene blue (MB) was selected as a probe compound to evaluate the catalytic activities of hemin-MWCNTs with H_2O_2 as oxidant. Electron paramagnetic resonance (EPR) technology combined with different scavengers, such as radical scavenger, electron capture agents were employed to investigate the mechanism of the positive effect of PFRs in MWCNTs. The findings of this study provide a new insight into the PFRs-enhanced catalytic performance and initiates an inspiring research domain of PFRs in catalysis field.

2. Experimental

2.1. Materials and reagents

MWCNTs (lot no. OEAKE, 40–60 nm diameter) were Tokyo Chemical Industry Co., Ltd. Hemin (98 wt%) was purchased from Aladdin Reagent (Shanghai, China). Thionylchloride, *N*,*N*′-dimethylformamide (DMF), dimethyl sulfoxide (DMSO), *p*-phenylenediamine (*p*-PDA), *o*-phenylenediamine (*o*-PDA), 2,3-diamino phenazine (DAPN), hydrogen peroxide (30 wt%, Sinopharm Chemical Reagent Co., Ltd., Shanghai, China) were used as analytical reagents. Methylene Blue (MB), Basic Brilliant Green (BG), Acid Red 1 (AR1), Acid Orange 7 (AO7), Reactive Red X-3B (RR X-3B) and Reactive Brilliant Red 3BF (RR 3BF) were used as the model contaminants without further purification. The spin trapping reagent, 5,5-dimethyl-pyrroline-oxide (DMPO) was supplied by Tokyo Chemical Industry Co., Ltd., Tokyo, Japan. Doubly distilled water was used throughout the contaminants decomposition process.

2.2. Catalyst preparation

MWCNTs was subjected to oxidizing, amidating, water washing and drying, and hemin-MWCNTs was prepared by immobilizing hemin on to *p*-phenylenediamine-functionalized MWCNTs through covalent bonding (see Supplementary material for a detailed description of the process). In the preparation process, *o*-MWCNTs, *p*-MWCNTs and hemin-MWCNTs represent oxidizing MWCNTs, *p*-phenylenediamine-functionalized MWCNTs, and *p*-phenylenediamine-functionalized MWCNTs supported hemin, respectively.

2.3. Analytical methods

The chemical structures of hemin and hemin-MWCNTs were analyzed with X-ray diffraction (XRD) (see Supplementary material for details). X-ray photoelectron spectroscopy (XPS) measurements were performed on a Kratos Axis Ultra DLD analyzer, and the standard Mg Kα (1256.6 eV) X-ray source operated at 10 mA and 15 kV. All binding energies were referenced to Au ($4f_{7/2}$) at 84 eV. Catalytic oxidation of dyes were carried out in a 20 mL glass beaker at 50 °C using H_2O_2 as oxidant under shaking condition. A typical reaction mixture contained the following initial concentrations: (a) dyes (50 μM, 20 mL); (b) supported catalyst hemin-MWCNTs (1 g/L, containing 61 μM hemin) or hemin (61 μM); and (c) oxidant H_2O_2 (50 mM). At given time-points, samples were passed through 0.22 μm pore size cellulose filters and analyzed immediately with a UV–vis spectrometer (Hitachi U-3010) by measuring the removal of dyes at the maximal wavelength. EPR signals of radicals trapped by DMPO were recorded at ambient temperature on a Bruker A300 spectrometer. The settings for the EPR spectrometer were as follows: center field, 3520 G; sweep width, 100 G; microwave frequency, 9.77 GHz; modulation frequency, 100 kHz; power, 20.00 mW. The total number of electrons released during the oxidation in the system was detected by the ABTS method.

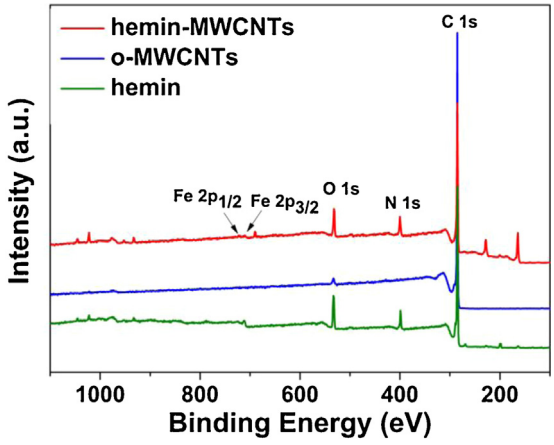

Fig. 1. XPS spectra of hemin, *o*-MWCNTs and hemin-MWCNTs.

3. Results and discussion

3.1. Characterization of hemin-MWCNTs

In this work, the bonding forms of hemin-MWCNTs were characterized using X-ray diffraction XRD (for detail, see Supplementary material) and X-ray photoelectron spectroscopy (XPS).

As shown in Fig. 1, compared with the spectrum of *o*-MWCNTs, the new bands of iron and nitrogen in the spectrum of hemin-MWCNTs were detected with a marked increase of oxygen. Moreover, according to full half-widths of the N1s peaks in hemin (Fig. 2A), N1s peaks occurring at 398.4 eV and 400.1 eV were attributed to four chemically equivalent N atoms, which binded to the central iron atom in the porphyrin ring [23]. No N1s signal was detected in *o*-MWCNTs (Fig. 2B); nevertheless, the spectra of N1s presented a different aspect when hemin was immobilized on MWCNTs. Besides the peaks of N1s (398.4 eV) and (400.1 eV) in hemin, the peak at 401.4 eV (Fig. 2C) might be explained by the nitrogen of amide group (—NH—CO—) being used for bonding between the carboxyl and substituted amino ($—NH_2$) groups. Furthermore, the O1s peaks gave coincident information about the bonding environment of hemin-MWCNTs (Fig. 3). For *o*-MWCNTs, the 531.7 eV peak and the 533.3 eV peaks were assigned to oxygen in a C═O double bond and a single bond of the hydroxyl group (C—O—H) (Fig. 3A), respectively. However, the proportion of C—O—H peaks was much smaller in hemin-MWCNTs (Fig. 3B), indicating that a part of the C—O—H was consumed by the amidation reaction. These results suggested that hemin was supported on MWCNTs covalently via amide linkage.

3.2. Oxidative removal of MB

Methylene blue (MB), a representative cationic dye, is widely used as a stain by many industries and the chemical structure of MB are shown in Fig. S3. In this study, MB was selected as

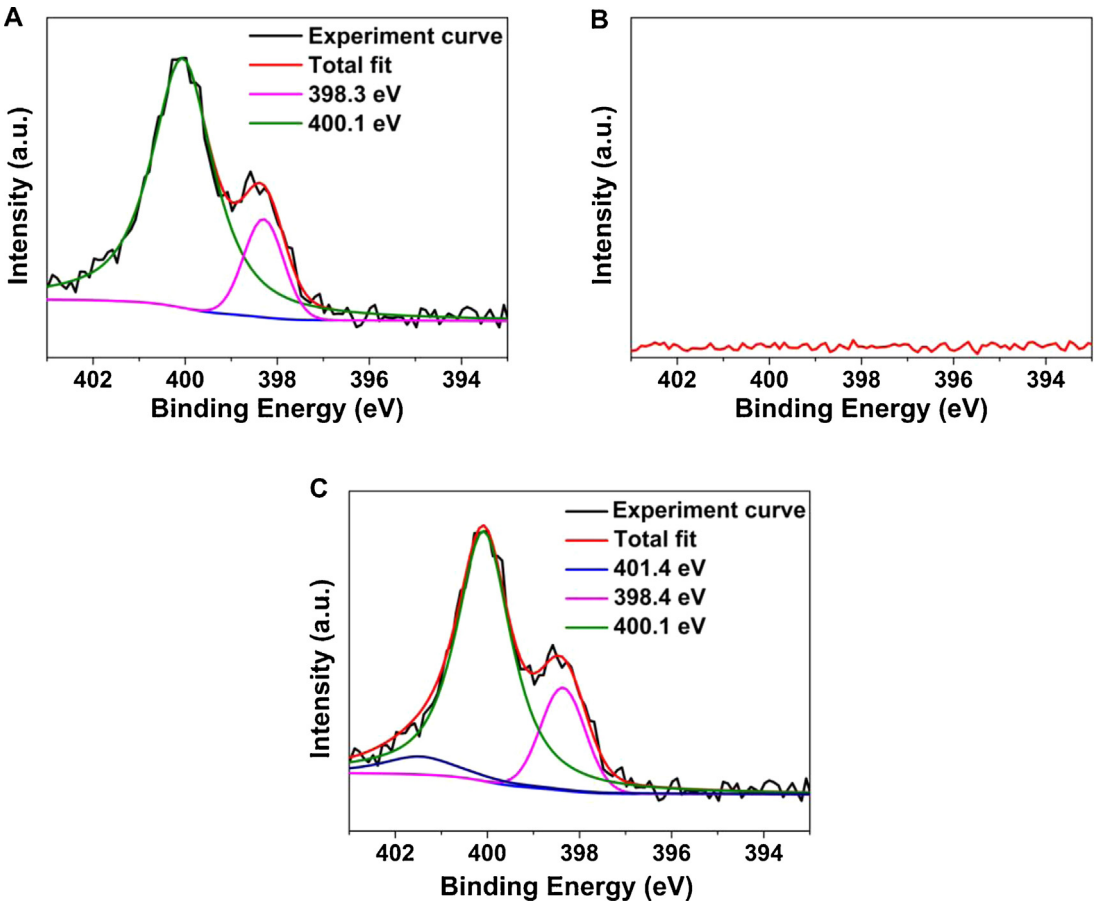

Fig. 2. XPS spectra of N 1s on (A) hemin, (B) *o*-MWCNTs, (C) hemin-MWCNTs.

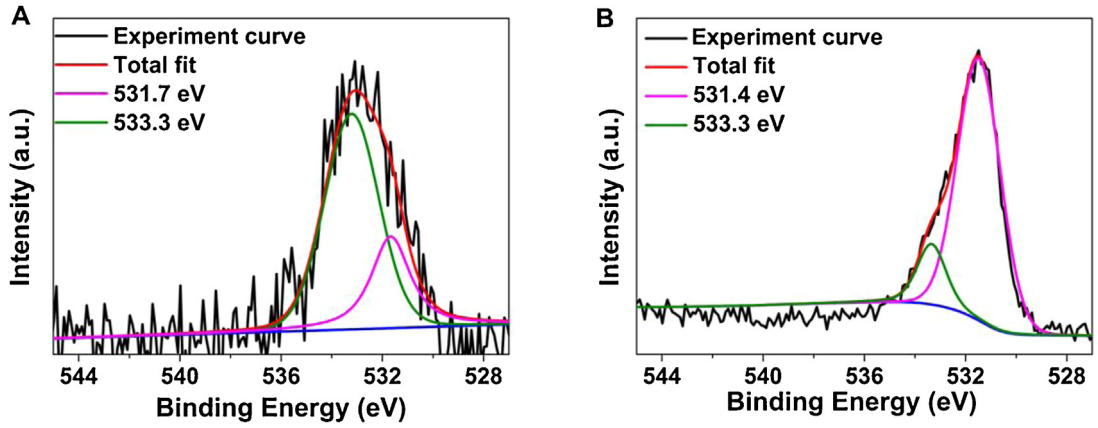

Fig. 3. XPS spectra of O 1s on (A) *o*-MWCNTs, (B) hemin-MWCNTs.

the probe compound to evaluate the catalytic activity of hemin-MWCNTs. As shown in Fig. 4C, H_2O_2 alone could barely decompose MB, suggesting that MB was stable in the presence of H_2O_2. When hemin and H_2O_2 were present, the concentration of MB was almost constant in 60 min, indicating that hemin could hardly activate H_2O_2 for the oxidation of MB. In the presence of hemin-MWCNTs, about 26% of MB was adsorbed onto hemin-MWCNTs. Surprisingly, when MWCNTs were introduced to hemin/H_2O_2, MB decomposition took place quickly, and about 98% of MB was removed under the same condition, suggesting that the introduction of MWCNTs significantly enhanced the catalytic oxidation. The intensity of MB UV–vis absorption peaks is shown in Fig. 4B and results were also demonstrated by the photo image (Fig. 4A). Furthermore, all of the MB decomposition curves obeyed pseudo-first-order kinetics (Fig. 4D). The MB decomposition rate constant was calculated to be 0.04195 min^{-1} in the hemin-MWCNTs/H_2O_2 system, which was almost 61 times that (0.00068 min^{-1}) in the hemin/H_2O_2 system, 155 times that (0.00027 min^{-1}) in the presence of H_2O_2.

On the basis of the above experimental results, it was found that hemin-MWCNTs/H_2O_2 system showed an extreme rate enhancement in oxidative decomposition of MB. In addition, we conducted an experiment to further investigate the catalytic activity of hemin-MWCNTs for catalytic oxidation of other organic dyes including Basic Brilliant Green (BG), Acid Red 1 (AR1), Acid Orange 7 (AO7),

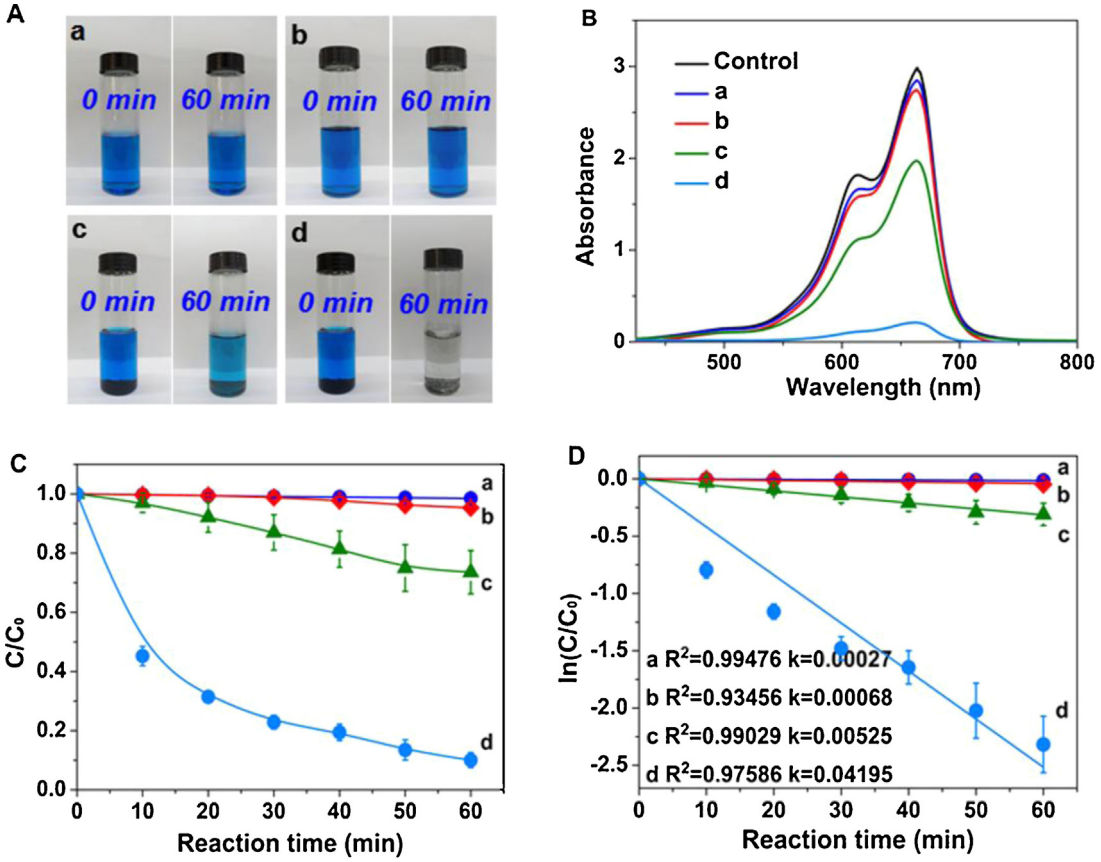

Fig. 4. (A) The digital picture of MB decolorization at 0 min and 60 min for different systems; (B) UV–vis spectra of MB removal by different systems within 60 min. (C) Time profiles of MB elimination under different system. (D) Plots of $\ln(C/C_0)$ versus time for the MB elimination in different systems. Conditions: (a) H_2O_2; (b) hemin/H_2O_2; (c) hemin-MWCNTs; (d) hemin-MWCNTs/H_2O_2, [MB] = 50 μM, [H_2O_2] = 50 mM, [hemin-MWCNTs] = 1 g/L, [hemin] = 61 μM, pH 7, at 50 °C.

Reactive Red X-3B (RR X-3B) and Reactive Brilliant Red 3BF (RR 3BF), as shown in Fig. 5. From Fig. 5, none of dyes were effectively removed in hemin/H_2O_2 system, while in hemin-MWCNTs/H_2O_2 system, all these dyes were effectively removed in 60 min, and the removal rates were higher than 95.0%. These results suggested that the hemin-MWCNTs/H_2O_2 system could also remove the representative dyes such as acid dyes, reactive dyes and basic dyes, which is significant to be applied in environmental remediation.

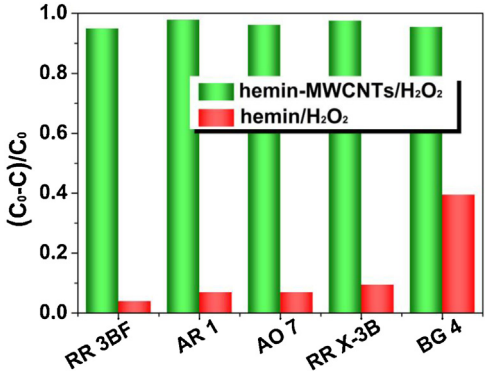

Fig. 5. Catalytic oxidation of different dyes under different conditions. Conditions: [H_2O_2] = 50 mM, [hemin-MWCNTs] = 1 g/L, [hemin] = 61 μM, pH 7, at 50 °C.

3.3. Mechanism in the catalytic system

Isopropyl (IPA) was reported to be a common •OH radical scavenger [24], which was employed to determine whether hydroxyl radicals were generated during the oxidation process. As shown in Fig. 6A, when excess IPA was added into hemin-MWCNTs/H_2O_2 system, the removal rate of MB decreased from 97.2% to 22.1%, suggesting that •OH played an important role during the oxidation process. However, it should be noted that the excess IPA did not completely inhibit the elimination of MB, implying that other active species may be involved in this catalytic reaction.

It has been reported that sulfoxides (e.g., dimethyl sulfoxide, methyl phenyl sulfoxide, and methyl *p*-tolyl sulfoxide) can react with Fe(IV) species to produce corresponding sulfones [25], which differed distinctly from their •OH involved products. In this work, dimethyl sulfoxide (DMSO) was used as a probe compound. As shown in Fig. 6B, the absorbance at 207 nm in the UV–vis spectroscopy of oxidation products of DMSO by hemin-MWCNTs/H_2O_2 (curve b) was greater than that of hemin/H_2O_2 (curve a), and the amount of hemin(Fe^{IV}=O) in two systems were also investigated (Fig. 6C). Compared with hemin, hemin-MWCNTs could react with H_2O_2 to produce more hemin(Fe^{IV}=O) due to the introduction of MWCNTs. These results indicated that hemin(Fe^{IV}=O) might participate in the catalytic removal of MB by hemin-MWCNTs.

An EPR spin-trapping technique was employed to further investigate the possible active species in the reaction. As shown in Fig. 6D, it was observed that the 4-line EPR spectrum characteristic of DMPO-•OH adducts were detected in aqueous solution. Moreover, the intensity of DMPO-•OH in the hemin-MWCNTs/H_2O_2 system was obviously higher than that in the hemin/H_2O_2 system, suggesting that a greater amount of •OH was generated than hemin/H_2O_2 system. In general, the hemin-MWNTs/H_2O_2 system generated higher ROS (hemin(Fe^{IV}=O) and •OH) than that in hemin/H_2O_2

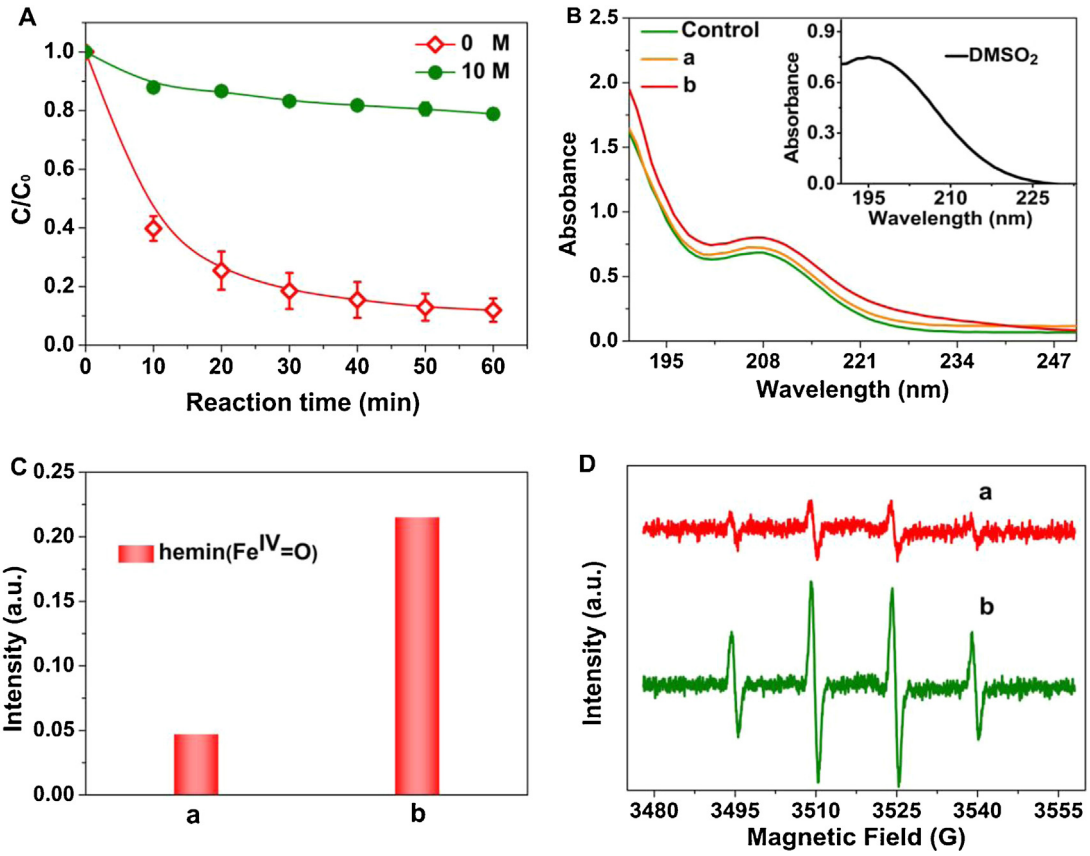

Fig. 6. (A) Effect of isopropyl on the catalytic reaction. (B) UV–vis spectra of spectroscopy of oxidation products of DMSO. Control: oxidation products of DMSO by H_2O_2, (a) oxidation products of DMSO by hemin/H_2O_2, (b) oxidation products of DMSO by hemin-MWCNTs/H_2O_2. The inset shows the absorption spectrum of 1 mM $DMSO_2$ aqueous solution. (C) Hemin (Fe^{IV}=O) amounts calculated according to DMSO method. (D) EPR spectra of DMPO-•OH adducts in aqueous solution in hemin-MWCNTs/H_2O_2 and hemin/H_2O_2 system. Conditions: [MB] = 50 μM, [DMSO] = 1 mM, [DMPO] = 10 mM, [hemin-MWCNTs] = 1 g/L, [hemin] = 61 μM, pH 7 (A, D, [H_2O_2] = 50 mM, at 50 °C; B, C, [H_2O_2] = 20 μM, after 10 min of reaction at ambient temperature).

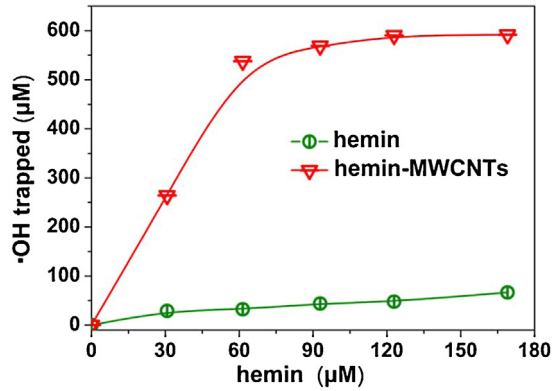

Fig. 7. Effect of hemin contents on •OH trapped in hemin/H_2O_2 and hemin-MWCNTs/H_2O_2. Conditions: [H_2O_2] = 50 mM, [OPDA] = 3 mM, pH 7, at 50 °C, reaction time: 12 min.

system, indicating that the introduction of MWCNTs was mainly responsible for the greatly enhanced formation of ROS.

The *o*-phenylenediamine (OPDA) method [26] was used to quantitatively investigate the generation of •OH in hemin/H_2O_2 and hemin-MWCNTs/H_2O_2. As illustrated in Fig. 7, the trapped •OH increased with the increase of hemin concentration, indicating that hemin contributed to more •OH formation. When 2.77 g/L hemin-MWCNTs (containing 169 μM hemin) was present, the amount of trapped •OH by OPDA was about 600 μM, which was much higher than that (65 μM) in hemin/H_2O_2. Obviously, the total number of •OH generated in the hemin-MWCNTs/H_2O_2 system was greater than that generated in the hemin/H_2O_2 system, which was consistent with the result in Fig. 6D.

The above results showed that the introduction of MWCNTs to hemin/H_2O_2 system significantly enhanced the formation of •OH, thus accelerating the MB elimination. Therefore, it is necessary to deeply investigate the role of MWCNTs in the •OH production process. In general, •OH production correlates with electrons released during the oxidation process [27]. Herein, the ABTS method was used to detect the total number of electrons released during the oxidation process in the hemin/H_2O_2 and hemin-MWCNTs/H_2O_2 systems [28]. Expectedly, it was found that the amounts of detected electrons in hemin-MWCNTs/H_2O_2 system were much greater than that in the hemin/H_2O_2 system (Fig. 8A), suggesting that MWCNTs enhanced the number of the released electron. Furthermore, considering PFRs in MWCNTs might influence electron transfer during the oxidation process, electron paramagnetic resonance (EPR) experiment was conducted to investigate the changes of PFRs. As shown in Fig. 8B, it was obviously observed that the signal intensity of PFRs in the MWCNTs decreased over time, meanwhile, conversion of hemin (Fe^{III}) to hemin (Fe^{II}) in hemin-MWCNTs was evidenced by XPS (Fig. S4). Furthermore, from the perspective of electrochemistry, the mechanism of electron transfer processes in the hemin-MWCNTs/H_2O_2 system was also investigated (Scheme S1). These results indicated that electron might transfer from PFRs to hemin, accelerating the reaction rate-determining step of hemin (Fe^{III}) to hemin (Fe^{II}), resulting in the enhanced ROS formation.

To further investigate the electron donating behavior of MWCNTs during the oxidation process, the change of structure of

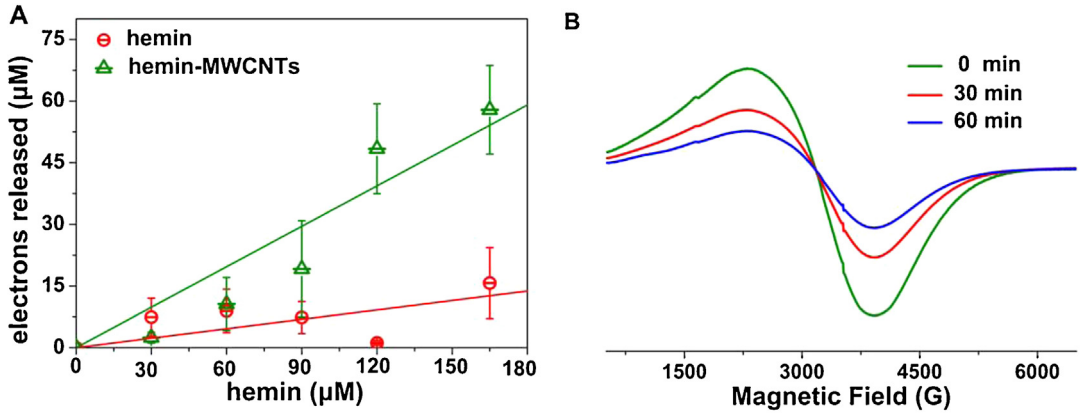

Fig. 8. (A) Effect of hemin contents on electrons released in hemin/H_2O_2 and hemin-MWCNTs/H_2O_2 during oxidation process; (B) EPR spectra of hemin-MWCNTs at different reaction time under room temperature. Conditions: [H_2O_2] = 50 mM, [hemin-MWCNTs] = 1 g/L,[ABTS] = 175 μM, pH 7, at 50 °C.

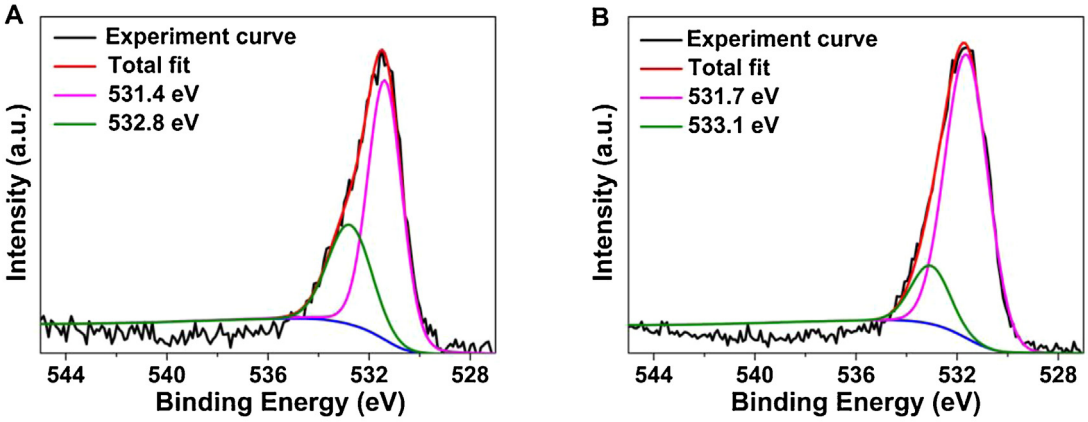

Fig. 9. XPS spectra of O1s on (A) fresh hemin-MWCNTs, (B) hemin-MWCNTs after utilization in the hemin-MWCNTs/H_2O_2 system.

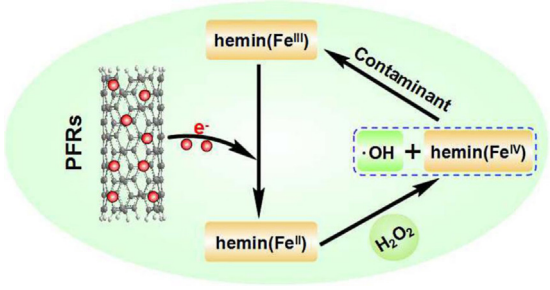

Scheme 1. The proposed catalytic mechanism in the hemin-MWCNTs/H_2O_2 system.

hemin-MWCNTs after utilization was measured by XPS. As shown in Fig. 9A, for the fresh hemin-MWCNTs, the O 1s peaks at 531.4 eV and at 532.8 eV were assigned to oxygen in a C=O double bond and oxygen in a single bond of the hydroxyl group (—O—H), respectively. However, after utilization, the intensity of oxygen in —O—H decreased obviously companying by an increase of the intensity of oxygen in C=O, suggesting that the part of C—O—H transferred into C=O, which might be attributed to electron transfer from PFRs to hemin. The corresponding proposed mechanism was depicted in Eqs. (s1) and (s2) (see Supplementary material).

Based on all the experimental results, a speculative mechanism of removal of contaminant in the hemin-MWCNTs/H_2O_2 system was proposed. As shown in Scheme 1, PFRs (MWCNTs) played a key role during the oxidation process, sustainably supplying electrons to hemin, which significantly accelerating the rate-determining conversion of hemin (Fe^{III}) to hemin (Fe^{II}), resulting in strongly enhanced formation of ROS (•OH and hemin(Fe^{IV}=O)), further promoting the removal of contaminant.

4. Conclusion

In the present study, the persistent free radicals of multiwalled carbon nanotubes (MWCNTs) were introduced into hemin system, constructing a novel and highly efficient heterogeneous catalytic system, hemin-MWCNTs/H_2O_2. This system brought about 61 times higher reaction rate in the decomposition of MB than that of the sole hemin/H_2O_2 system, which was attributed to the more ROS (•OH and hemin(Fe^{IV}=O)) formation. It was found that the PFRs concentrations in MWCNTs markedly decreased, accompanying by the more trapped electrons. Moreover, on the basis of the online electrochemical and XPS measurements in the hemin-MWCNTs/H_2O_2 system indicated that electron might transfer from PFRs to hemin, accelerating the conversion of hemin (Fe^{III}) to hemin (Fe^{II}), resulting in more ROS production. This research provides a new insight into the PFRs-enhanced catalytic performance and open up an inspiring research domain of PFRs in catalysis field.

Acknowledgments

This work was supported by the State Key Program of National Natural Science of China (No. 51133006), the National Natural Science Foundation of China (No. 51302246), the Natural Science Foundation of Ningbo (No. 2015A610047) and Zhejiang Provin-

cial Natural Science Foundation of China (No. LY14E030015 and LQ15E030005).

Appendix A. Supplementary data

Supplementary data associated with this article can be found, in the online version, at http://dx.doi.org/10.1016/j.apcatb.2015.10.051.

References

[1] Y.H. Lin, J.S. Ren, X.G. Qu, Acc. Chem. Res. 47 (2014) 1097–1105.
[2] W.D. Woggon, Acc. Chem. Res. 38 (2005) 127–136.
[3] R. Qu, L.L. Shen, Z.H. Chai, C. Jing, Y.F. Zhang, Y.L. An, L.Q. Shi, ACS Appl. Mater. Interfaces 6 (2014) 19207–19216.
[4] R.T. Tom, T. Pradeep, Langmuir 21 (2005) 11896–11902.
[5] T.C. Bruice, Acc. Chem. Res. 24 (1991) 243–249.
[6] Y. Zang, J.P. Lei, L. Zhang, H.X. Ju, Anal. Chem. 86 (2014) 12362–12368.
[7] S.Y. Deng, J.P. Lei, Y. Huang, Y. Cheng, H.X. Ju, Anal. Chem. 85 (2013) 5390–5396.
[8] M.S. Mizrachi, G.M. Pavan, E. Levin, A. Danani, N.G. Lemcoff, J. Am. Chem. Soc. 133 (2011) 14359–14367.
[9] S. Bhattacharjee, T.J. Dines, J.A. Anderson, J. Catal. 225 (2004) 398–407.
[10] M. Duan, J. Li, G. Mele, C. Wang, X. Lü, G. Vasapollo, F. Zhang, J. Phys. Chem. C 114 (2010) 7857–7862.
[11] V.P. Barros, A.L. Faria, T.C.O. MacLeod, L.A.B. Moraes, M.D. Assis, Int. Biodeterior. Biodegrad. 61 (2008) 337–344.
[12] Y. Huang, W. Ma, J. Li, M. Cheng, J. Zhao, J. Phys. Chem. B 107 (2003) 9409–9414.
[13] Q. Wang, Z. Yang, X. Zhang, X. Xiao, C.K. Chang, B. Xu, Angew. Chem. Int. Ed. 119 (2007) 4363–4367.
[14] F. Bedioui, Coord. Chem. Rev. 144 (1995) 39–68.
[15] L. Khachatryan, E. Vejerano, S. Lomnicki, B. Dellinger, Environ. Sci. Technol. 45 (2011) 8559–8566.
[16] L. Khachatryan, B. Dellinger, Environ. Sci. Technol. 45 (2011) 9232–9239.
[17] G.D. Fang, J. Gao, C. Liu, D.D. Dionysiou, Y. Wang, D. Zhou, Environ. Sci. Technol. 48 (2014) 1902–1910.
[18] A. Valavanidis, N. Iliopoulos, G. Gotsis, K. Fiotakis, J. Hazard. Mater. 156 (2008) 277–284.
[19] S. Gahlot, V. Kulshrestha, ACS Appl. Mater. Interfaces 7 (2015) 264–272.
[20] S.J. Jiang, S.Q. Song, Appl. Catal. B: Environ. 140–141 (2013) 1–8.
[21] B. Gao, C. Peng, G.Z. Chen, G.L. Puma, Appl. Catal. B: Environ. 85 (2008) 17–23.
[22] D. Baskaran, J.W. Mays, X.P. Zhang, M.S. Bratcher, J. Am. Chem. Soc. 127 (2005) 6916–6917.
[23] G. Faubert, G. Lalande, R. Côté, D. Guay, J.P. Dodelet, L.T. Weng, P. Bertrand, G. Dénès, Electrochim. Acta 41 (1996) 1689–1701.
[24] P. Kormali, T. Triantis, D. Dimotikali, A. Hiskia, E. Papaconstantinou, Appl. Catal. B: Environ. l68 (2006) 139–146.
[25] S. Pang, J. Jiang, J. Ma, Environ. Sci. Technol. 45 (2011) 307–312.
[26] Y. Fang, A. Deng, Y. Huang, Chin. Chem. Lett. 20 (2009) 1235–1240.
[27] S.E. Page, M. Sander, W.A. Arnold, K. McNeill, Environ. Sci. Technol. 46 (2012) 1590–1597.
[28] S.E. Page, G.W. Kling, K.H. Sander, J.R. Harrold, K. Logan, R.M. Cory, Environ. Sci. Technol. 47 (2013) 12860–12867.